Two-Photon Decay in Heavy Atoms and Ions

P. H. Mokler[1] and R. W. Dunford[2]

[1] GSI, D-64291 Darmstadt, Germany
[2] Argonne National Laboratory, Argonne, Illinois 60439, USA

Abstract

We review the status of and comment on current developments in the field of two-photon decay in atomic physics research. Recent work has focused on two-photon decays in highly-charged ions and two-photon decay of inner-shell vacancies in heavy neutral atoms. We emphasize the importance of measuring the shape of the continuum emission in two-photon decay as a probe of relativistic effects in the strong central fields found in heavy atomic systems. New experimental approaches and their consequences will be discussed.

1. Introduction

Two-photon decay was first discussed by Maria Göppert-Mayer in 1929 [1,2]. The initial interest in this decay mode was in the field of astrophysics [3,4] since this process contributes to the continuum radiation from planetary nebulae [4]. The main interest at the present time is in comparisons between theoretical calculations and laboratory experiments in heavy atoms and ions where strong central field strengths prevail.

Breit and Teller [5] were the first to estimate the two-photon decay rates of the low-lying levels of hydrogen and helium. They confirmed the prediction by Göppert-Mayer that the $2\,^2S_{1/2}$ state in hydrogen decayed primarily by emission of two electric-dipole (2E1) photons. Subsequently, nonrelativistic calculations for the dominant 2E1 decay mode of the $2\,^2S_{1/2}$ state for one-electron ions were made by Spitzer and Greenstein [4], Shapiro and Breit [6], Zon and Rapoport [7], Klarsfeld [8,9], and Drake [10]. The lifetime for two-photon decay was found to be about $1/7$ s and decreases as Z^{-6} as a function of the nuclear charge Z of a one electron ion. The nonrelativistic formula for the 2E1 two-photon decay rate with one photon having a frequency between ν_1 and $\nu_1 + d\nu_1$ has the form [11]:

$$A(\nu_1)\,d\nu_1 = \frac{2^{10}\pi^6 e^4}{h^2 c^6} \nu_1^3 \nu_2^3 |M_{fi}|^2 \,d\nu_1. \tag{1}$$

The transition matrix element is given by:

$$M_{fi} = \hat{\varepsilon}_1 \cdot \hat{\varepsilon}_2 \sum_n z_{fn} z_{ni} \left(\frac{1}{\nu_{ni} + \nu_2} + \frac{1}{\nu_{ni} + \nu_1} \right) \tag{2}$$

where ε_i are the polarization vectors for photons 1 and 2, the index n refers to intermediate p-states, z_{fn} and z_{ni} are electric dipole matrix elements, and the sum is over all discrete and continuum states. The photons emitted in this process form a continuum, but the sum of the energies of the two coincident photons from each decay is equal to the

transition energy. The total decay rate is given by

$$A_T = \tfrac{1}{2} \int_0^{\nu_0} A(\nu_1)\,d\nu_1 \tag{3}$$

where ν_0 is the transition energy. The factor $1/2$ comes because photon 1 is counted twice in the interval $\{0, \nu_0\}$. For the H-like $2\,^2S_{1/2}$ level, as the nuclear charge Z increases, the dipole matrix elements decrease as $1/Z$ whereas the frequencies ν_n increase as Z^2 so that the overall decay rate increases as Z^6. Eichler [12] showed that the form of the transition rate given by Eqs. (1–3) which is similar to that given by Göppert-Mayer, includes the so-called A^2 term (here A is the vector potential) in the nonrelativistic interaction Hamiltonian. This cleared up some confusion about whether this term had been neglected in early theoretical treatments of two-photon decay.

For H-like systems the two-photon decay mode dominates at low Z but the relativistic M1 decay becomes more probable at high Z. The spectral distribution for the two-photon decay was predicted to form a broad continuum with a maximum at half the transition energy which gradually drops to zero at the endpoints. The opening angle θ between the two photons has a $(1 + \cos^2\theta)$ distribution which is symmetric about the minimum at $\theta = 90°$. The opening angle correlation is sketched in Fig. 1. Au [13] found that this result was only approximate. He studied the effect of including higher multipoles in the calculation and showed that it caused an asymmetry about $\theta = 90°$ in the angular correlation between the two photons of order $(\alpha Z)^2$. In other work, Tung et al. [14] studied two-photon decay between arbitrary states (n, l, m) of hydrogenic systems and Florescu et al. [15,16] made a systematic study of $ns \rightarrow 1s$ and $nd \rightarrow 1s$ two-photon transitions. A general discussion of selection rules for 2E1 two-photon transitions is given by Bonin and McIlrat [17].

There are a number of two-photon transitions of interest in He-like systems. In Fig. 2 a level diagram with the different possible transitions is shown for heavy He-like ions. Dalgarno [18,19] made the first detailed calculation of the two-photon decay of the $2\,^1S_0$ level for helium (nonrelativistic). Other nonrelativistic calculations for this case have been done by Victor [20,21], Jacobs [22], and Drake [10,23]. Since the initial and final electronic states have zero angular momentum, the M1 branch is absent even in the relativistic limit. The relevant formulas for the decay rate are the same as in the H-like case (See Eqs. (1–3)). The spectral shape and opening angle distributions are also similar to those obtained for the $2\,^2S_{1/2}$ level in H-like ions.
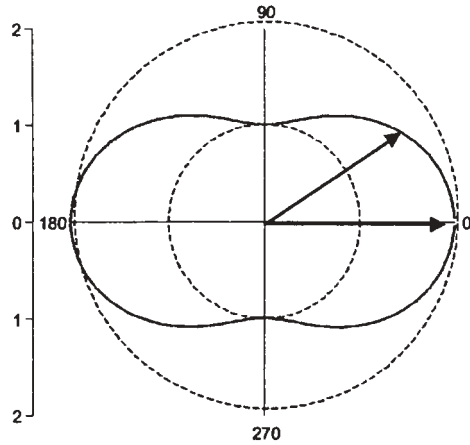
Fig. 1. Angular distribution on the opening angle between the two photons for an $s \to s$ transition in 2E1 decay; $(1 + \cos^2 \theta)$ angular correlation.
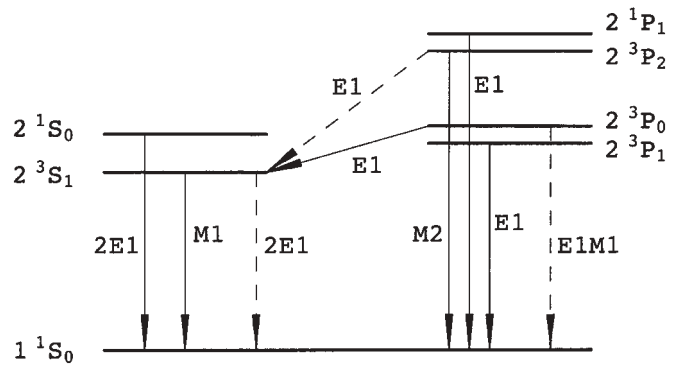

Fig. 2. Level diagram for heavy He-like ions. Multipolarities for the most probable decay modes are indicated by solid arrows. Weaker decay modes are shown as dashed arrows. (Not to scale.)

Although the $1s2s\,^3S_1$ level in He-like ions decays to the ground state predominantly by single-photon M1 emission, it has a small branch to decay via two photons. This process has been analyzed theoretically by Bely and Faucher [24,25] and by Drake *et al.* [23,26]. Bely and Faucher's results extend from $Z = 2$ to $Z = 31$. The branching ratio for double-photon decay is small throughout this range, the largest value is 5×10^{-4} for $Z = 31$. The spectral shape of the continuum emission in the $^3S_1 \to {}^1S_0$ transition is markedly different from that of $2\,^1S_0$ or H-like $2\,^2S_{1/2}$ decays. As a consequence of the fact that photons obey Bose-Einstein statistics, atomic 2E1, $J = 1 \to J' = 0$ amplitudes are forbidden for photons of the same energy [17,27]. As a result, the continuum distribution of the two-photon decay of the $^3S_1$ level is suppressed at the midpoint where the two photons would share the transition energy equally. The distribution in the photon opening angle θ has the form $1 - (1/3)\cos^2 \theta$, which has a maximum at $\theta = 90°$ in contrast to the angular distribution for decay of the $2\,^1S_0$ level which has maxima at $\theta = 0°$ and $180°$. To date, the two photon decay of the $2\,^3S_1$ level in He-like ions has not been observed.

At low-Z, the $2\,^3P_0$ level in He-like ions decays to the $2\,^3S_1$ level via single photon electric dipole decay but it can also decay to the ground state by emission of two photons. This two-photon transition involves both E1 and M1 couplings and it becomes important at high Z. Drake [28] calculated the E1M1 two-photon transition probability for decay of the $2\,^3P_0$ level of uranium and found that this state decays 30% of the time via emission of two photons. More recently, Savukov and Johnson [29] calculated the E1M1 transition rates for helium like ions in the rage $Z = 50$ to $Z = 94$. They also present corrected values of the lifetimes of the $2\,^3P_0$ levels in these ions. The fraction of the time that the $2\,^3P_0$ state decays via E1M1 two photon emission varies from 0.2% at $Z = 50$ to 37% at $Z = 94$. The spectral shape has a local maximum at the center of the distribution and rises in the wings [29]. Two-photon decay of the $2\,^3P_0$ state has been discussed in connection with measurement of parity nonconservation in high-Z helium like ions [30]. Schmieder [31] has discussed double- and triple-photon decay of the $2\,^3P_0$ level in Be-like ions. To date, none of these exotic decay modes of triplet He-like and Be-like ions has been observed.

The first laboratory observation of two-photon decay was made by Novick *et al.* [32–34] in the decay of the $2\,^2S_{1/2}$ level of singly ionized helium. Many of the early two-photon decay experiments focused on measuring the lifetimes of the two-photon-emitting states using mainly beam-foil-spectroscopy methods. The lifetime of the $2\,^2S_{1/2}$ level in H-like ions has been measured for a number of ions in the range $Z = 1$ to $Z = 47$ [35–45], with results at the level of 1% being reported for Ar^{17+} [38] and Ni^{27+} [35]. The lifetime of the $2\,^1S_0$ level in He-like ions has been measured from $Z = 2$ to $Z = 41$ [11,35,36,38,44–49]. The most precise measurements have been made in Kr^{34+} [46], Br^{33+} [49], and Ni^{26+} [35] where uncertainties of about 1% have been reported.

Two-photon decay has also been studied in the decay of K-holes in neutral atoms. Freund first suggested that two-photon transitions between inner-shell vacancy states in neutral atoms could be observable [50]. He found that the branching ratios were about 10^{-6} of the single photon transition probabilities. Following this work, a number of theoretical studies, both nonrelativistic [12,51–53] and relativistic [54,55], have been reported. An early question about the theory concerned whether or not to include the occupied bound states of the atom in the sum over intermediate states. Guo [56] proved that the Pauli exclusion principle does not prohibit summing over all intermediate states including occupied bound states. If such occupied states lie between the initial and final states (e.g., the 2p state in the two-photon transition $3d \to 1s$) then there is a large increase in the differential transition probability ("intermediate-state resonance") when the energies of the photons approach the values of a cascade decay via these levels.

The first observation of two-photon decay from inner-shell-vacancy states was made by Bannett and Freund [52,57] measuring fast photon coincidences between two solid state (Si-Li) X-ray detectors. Inner-shell vacancies were produced by irradiating a thin Mo foil with Ag X-rays from a sealed X-ray tube. They observed both $2s \to 1s$ and $3d \to 1s$ decays in molybdenum. The continuum shape was not well determined as the measurements were made over a restricted energy range near the midpoint of the distribution.

Ilakovac *et al.* [58–60] used radioactive sources to generate K vacancies in xenon, silver and hafnium and studied the two-photon decays of these excited atoms. They

used a pair of high purity germanium detectors and also applied the photon coincidence technique. Two-photon emission in the transitions 2s → 1s, 3s → 1s, 3d → 1s, and 4s, 4d → 1s were observed and compared with the various theoretical calculations. They found general agreement with the expected continuum shapes and, in particular, the single photon spectra of the 3d → 1s transitions in silver and hafnium confirmed the predicted intermediate-state resonance effect and supported Guo's assertion about the need to include the occupied levels in the sum over the intermediate states. If the occupied states (in particular the 2p states) are not included in the sum over intermediate states, the calculation of the transition probability exhibits a maximum at the midpoint of the distribution [60].

The importance of two-photon decay in studying atomic structure is mirrored in the field of nuclear physics where it has provided useful information on nuclear structure. Two-photon emission has been observed in nuclear transitions in ^{40}Ca, ^{90}Zr [61] and ^{16}O [62] using the Heidelberg–Darmstadt "crystal ball". A surprising result of this research was that, in each case, the angular correlation between the two γ-rays was asymmetric about 90°. This was interpreted as arising from interference between the 2E1 and the 2M1 contributions to the transitions which were found to be of comparable strength. These experiments also made use of measurements of the spectral distribution of two-photon decay. The photon energy distribution was used to determine the pure dipole nature of the two-photon decay of the first excited 0$^+$ state of ^{16}O [62]. The theory of nuclear 2-γ decay including treatment of higher multipolarities and angular correlations is discussed in an appendix to Ref. [62]. Equations (1–3) are applicable for nuclear two-photon decay where the nonrelativistic treatment is appropriate. For the nuclear transitions that have been studied to date, the second order matrix element M_{fi} contains contributions from only 2E1 and 2M1 amplitudes. For the 2E1 amplitude, the reduced matrix element is expressed in terms of a quantity called the transition polarizability α_{E1}; and the reduced matrix element for the 2M1 amplitude is proportional to a quantity called the transition susceptibility χ. The quantities α_{E1} and χ have no simple dependence on the transition energy and the overall dependence of the two-photon rate on transition energy comes through the factor $\nu_1^3 \nu_2^3$ in Eq. (1). After integrating over ν_1 (Eq. (3)) we get the useful result that for given magnitudes of α_{E1} and χ, the nuclear 2E1 and 2M1 two-photon transition rates increase as the seventh power of the transition energy ν_0^7.

In this article we focus on the more recent developments in the study of two-photon decay in atomic systems. These have generally involved studies of heavy ions and atoms where relativistic effects become important. Relativity modifies the structure of heavy atomic systems and, hence, influences the two-photon decay rates. Moreover, there higher multipole amplitudes may contribute non-negligibly to two-photon decay in heavy systems. We will discuss goals for future developments in the field of two-photon decay and will stress the importance of studying the spectral shapes and opening angle distributions. Such differential measurements provide a wealth of information to test the theoretical calculations. In Section 2 we consider recent work in the area of highly charged ions, in Section 3 we cover recent developments of two-photon decay of inner-shell vacancy states in heavy atomic systems, and then in Section 4 we conclude and point to future directions in this field.

2. Two-photon spectral shape in heavy ions

An important experimental issue in the study of two-photon decay in few-electron heavy ions is the detailed examination of the shape of the two-photon continuum. These systems have states which decay predominantly by emission of two photons, so that clean, high-precision experiments are possible. The theoretical calculations predict that the spectral distributions should depend on the nuclear charge but this fact has only recently been demonstrated experimentally.

Klarsfeld's nonrelativistic result for decay of metastable hydrogenic atoms ($2\,^2S_{1/2}$ level) after averaging over photon polarization gives for the triply differential two-photon probability [8,9]:

$$\frac{d^3 w_{2\gamma}}{dE_1\, d\Omega_1\, d\Omega_2} = Z^4 \alpha^6 \frac{2^5}{(2\pi)^3 3^8}(1+\cos^2\theta) f(1-f)\phi^2(f),$$

$$(4)$$

where θ is the opening angle between the two photons, Z is the nuclear charge, and f is the fraction of the transition energy $E_0 = E_1 + E_2$ carried by one of the photons. The function $\phi(f)$ involves a sum over intermediate bound and continuum states. The dependence on opening angle is completely factored in Eq. (4) for $d^3 w_{2\gamma}$. The total decay rate is obtained by integration over energy and photon emission angles and has an over all Z^6 dependence since the energy integration contributes with another factor of Z^2. Equation (4) indicates that, in the nonrelativistic limit, the spectral shape for two-photon decay of the H-like $2\,^2S_{1/2}$ state does not depend on Z. This is no longer true when relativistic effects are taken into account or in multi-electron atoms when electron-electron interactions are included.

In analyzing the two-photon decay of heavy ions we need to consider the relativistic formula for two-photon decay. In the notation of Goldman and Drake [63], the two-photon differential decay probability is given by (in atomic units):

$$d^3 w_{2\gamma} = \frac{\omega_1 \omega_2}{(2\pi)^3 c^2}\left|R_{fi}\right|^2 d\Omega_1\, d\Omega_2\, d\omega_1 \qquad (5)$$

where i and f refer to the initial and final states, ω_j is the frequency and $d\Omega_j$ is the solid angle for the jth photon. The transition energy ω_0 satisfies $\omega_0 = \omega_1 + \omega_2$. The second order matrix element R_{fi} is given by:

$$R_{fi} = \sum_n \frac{\langle f|\tilde{A}_2^*|n\rangle\langle n|\tilde{A}_1^*|i\rangle}{E_n - E_i + \omega_1} + \frac{\langle f|\tilde{A}_1^*|n\rangle\langle n|\tilde{A}_2^*|i\rangle}{E_n - E_i + \omega_2}. \qquad (6)$$

The sum is over all positive and negative energy solutions of the Dirac equation. For photon plane waves with propagation vectors $\boldsymbol{k}_j$ and polarization vectors $\hat{\boldsymbol{e}}_j$, the

operators are given by:

$$\tilde{A}_j^* = \alpha \cdot (\hat{e}_j + G\hat{k}_j)\,e^{-ik_j \cdot r} \tag{7}$$

where G is an arbitrary gauge parameter.

If we retain only the 2E1 contribution to the decay rate of the H-like $2\,^2S_{1/2} \rightarrow 1\,^2S_{1/2}$ and He-like $2\,^1S_0 \rightarrow 1\,^1S_0$ two-photon decays, the matrix element R_{fi} has no overall Z dependence (although it does have a complicated dependence on Z via the wave functions). For these transitions the overall Z dependence is contained in the factor $\omega_1\omega_2\,d\omega_1$ in Eq. (4). It is convenient to write this in terms of f, the fraction of the transition energy corresponding to ω_1:

$$\omega_1\omega_2\,d\omega_1 = \omega_0^3(1-f)f\,df. \tag{8}$$

The well-known Z^6 scaling for 2E1 two-photon decays follows from the fact that the transition energy ω_0 scales as Z^2. It is clear that it is the second order matrix element R_{fi} that contains the interesting physics in this problem and so it is useful to divide out the trivial "phase space" factor $(1-f)f$ from the two-photon continuum emission data and compare this with theoretical calculations of $|R_{fi}|^2$. We emphasize that the formula for the two-photon decay rate given in Eq. (1) is equivalent to Eq. (5) in the nonrelativistic limit but Eq. (1) is not as useful for studying the changes in the structure of the ions as a function of Z because in this case the overall Z dependence has not been factored out of the second order matrix element, Eq. (2).

Parpia and Johnson [64,65] and Goldman and Drake [63,66] have made fully relativistic calculations of the H-like decay rate. They found that when relativity is included in the atomic structure, the continuum shape was no longer independent of Z but exhibited an enhancement of the distribution near $f = 0.5$ relative to the wings of the distribution. For helium-like atoms, the atomic structure and hence the shape of the two-photon continuum varies with Z even in the nonrelativistic limit due to electron-electron correlations. Drake's results [67] for the continuum shapes of helium-like ions between $Z = 2$ and $Z = 36$ indicate a behavior opposite to that of the relativistic H-like shapes in that they become flatter as Z increases. This behavior is related to the difference in the scaling of the energy separations within the $n = 2$ shells. For the He-like case (at low Z) the energy separation is dominated by the electron–electron interaction and increases linearly as a function of Z. For H-like ions, the 2s-2p energy separations scale as Z^4 due to relativistic and QED effects. The energy separations 2s-np scale roughly as Z^2 in both species. So neglecting the matrix elements, the relative importance of the 2s-2p coupling increases in He-like ions as Z increases since $\Delta E(n=2)/\Delta E(n>2) \sim 1/Z$, whereas the 2s-2p coupling becomes less important for H-like ions as Z increases since for these ions $\Delta E(n=2)/\Delta E(n>2) \sim Z^2$. For heavy heliumlike ions, fully relativistic calculations of two-photon decay of the He-like $2\,^1S_0$ and $2\,^3S_1$ levels have been done by Derevianko and Johnson [68]. Their results corroborate the trend at low Z that the spectral shape becames flatter as Z increases, but at higher Z there is a reversal and the spectral distributions become narrower as Z is increased above 20. This is due to the fact that the relativistic corrections become more important than the electron-electron interactions at high Z.

The first observation of the continuum emission from He-like ions was made by Elton, Palumbo and Griem [69]. They observed a broad peak in a deuterium-neon plasma whose width and position agreed with that expected for the two-photon continuum of Ne IX. In other early work, rough verification of the shape of the continuum radiation from decay of metastable H-like atoms was made by Novick *et al.* [33] using He$^+$ and by O'Connell *et al.* [70] using hydrogen. They also made a rough verification of the $(1 + \cos^2\theta)$ angular correlation.

Marrus and Schmieder [36,71] used the beam-foil technique to study two-photon decay in highly charged ions. They observed the continuum radiation from decay of the $2\,^2S_{1/2}$ level in H-like argon and the $2\,^1S_0$ level in He-like argon using a pair of Si(Li) detectors looking face to face downstream on the excited ion beam. This method of applying coincident detection of both the photons has also been used to observe the two-photon continuum in H-like Ni [44], Kr [42] and Nb [45], and He-like Ni [44], Br [49], Kr [46] and Ag [45]. These experiments resulted in measurements of the lifetimes of the two-photon-emitting states but detailed measurements of the shapes of the continua were not attempted. The continuum radiation from two-photon decay was also observed in connection with studies of resonant transfer and excitation (RTE) in He-like Ge [72], and Kr [73–75]. These photon coincidence experiments pointed to a technique for selective excitation of the $2\,^1S_0$ level in He-like ions which could be important in future studies.

The more recent studies of two-photon decay in highly charged ions have been concerned with measurement of the spectral distribution of the continuum radiation in He-like ions. In contrast to lifetime measurements, a determination of the two-photon decay spectrum will provide a lot more information on the details of the atomic structure involved. The spectrum is symmetric with respect to both photons, i.e. mirror-symmetric around the mid point at half the total transition energy. The spectrum depends on the phase space factor $f(1-f)$ and the transition matrix element [76]. The latter varies considerably with the atomic system [10,64,68]. In particular for high Z in He-like systems, the strong central field will overwhelm the electron–electron interaction and relativistic effects will dominate the atomic structure. Here, both ^1P and ^3P intermediate states have to be included [68]. In Fig. 3 some reduced matrix elements (i.e., the matrix elements squared and the phase space factor $f(1-f)$ is already factored out) for 2E1 decay as function of f according to Derevianko and Johnson's calculations are shown. The phase space factor $f(1-f)$ is given by the shaded area in Fig. 3.

The first detailed study of the spectral shape of the two-photon decay in heavy He-like ions beyond $Z = 20$ was done at the ATLAS facility at Argonne National Laboratory near Chicago using Kr ions [77]. This two-photon coincidence measurement, done in a beam foil arrangement, confirmed the calculations of Drake [10] based on a non-relativistic approach. A clear change in the relative spectral distribution (normalized to the total transition
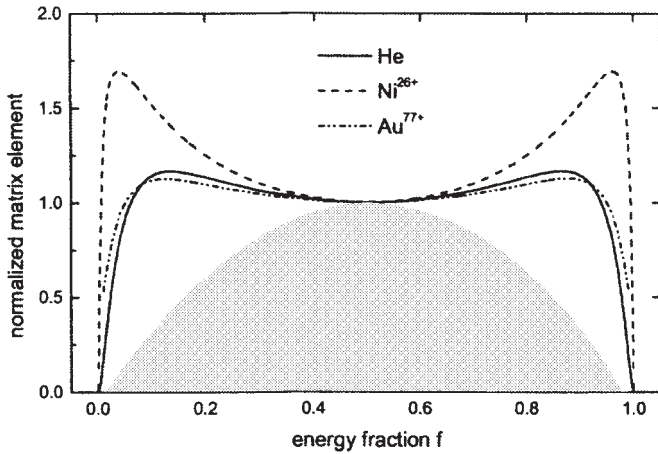
Fig. 3. Reduced matrix element for 2E1 transitions in He-like ions as a function of the normalized photon energy according to Ref. [68]. The rim of the shaded area represents the parabolic shape of the phase space factor.

energy) compared to the one expected for atomic He was established.

In a further investigation at ATLAS using Ni ions, the accuracy in determining the shape of the two-photon spectra caused by the uncertainties in the efficiencies was significantly improved by comparing the spectral distributions for the two-photon decays in H-like and He-like Ni ions [76]. In this experiment He-like Ni ions are incident on a thin carbon foil where some of the ions are excited to the metastable $2\,^1S_0$ level. X-rays emitted from ions just downstream of the foil are detected by an array of Si(Li) detectors. In Fig. 4 the spectrum from one of the detectors is shown. The two photon continuum denoted "2E1" is clearly seen on the low energy side of the single photon M1, M2 decay radiation from the He-like $n = 2$ levels $2\,^3S_1$ and $2\,^3P_2$. At low X-ray energy, transitions to higher shells (Balmer) are visible; the Mo fluorescence line comes from the shielding.

The two-photon events can be clearly separated from the backgrounds using the coincidence condition and requiring
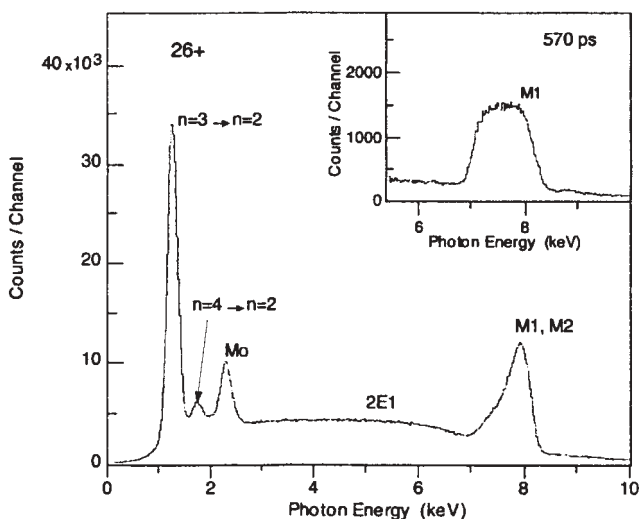

Fig. 4. Singles photon spectrum from one of the Si(Li) X-ray detectors with Ni^{26+} incident on a $10\,\mu g/cm^2$ C target. The detector looks behind the exciter foil (about 180 ps downstream) and is shielded from a direct view of the foil. The inset shows a spectrum taken with the foil moved upstream so that the flight time to the detectors is 570 ps where the M1 transition prevails.
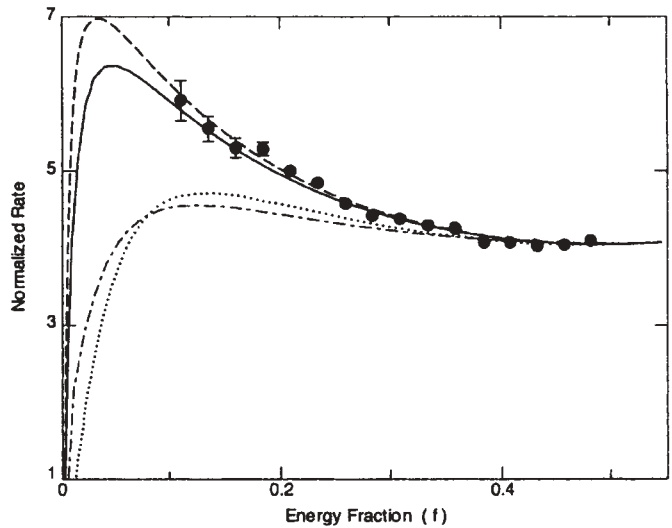

Fig. 5. Normalized rate for two-photon decay as a function of the photon energy (in units of the fraction of the transition energy). The data for He-like nickel are compared with various theoretical results including Drake's (dashed curve) nickel shape and Derevianko and Johnson's nickel (solid line), helium (dotted line), and Au (dot-dashed) spectral shapes. All data are normalized to the area under the last four data points. The data and theory have been divided by the phase space factor $f(1 - f)$ and are proportional to the reduced transition matrix element squared.

that the energy sum between each pair of detectors is equal to the sum-energy corresponding to the transition energy for the two-photon transition. Figure 5 shows the final result from the Ni spectral shape experiment. The reduced matrix element is plotted as a function of the relative energy f. The results show a large deviation from the spectral shapes for both light He atoms and very heavy He-like Au ions and agree well with the predictions for $Z = 28$; however, the data cannot distinguish between the relativistic and non-relativistic calculations for Ni.

At this medium Z value the measurements are still in accordance with both the non-relativistic calculations of Drake [10] and the full relativistic calculations of Derevianko and Johnson [68] as both approaches are not really at variance in that case. However, the accuracy of this measurement is so promising that for heavier atomic systems a clear distinction between the different calculations can be expected.

The heaviest He-like system probed so far in detail by the two-photon decay is Au [78]. At the heavy ion synchrotron facility SIS at GSI-Darmstadt He-like Au^{77+} ions were produced by stripping at 106 MeV/u and then excited in a thin Al foil. The emitted X-rays were detected by Ge(i) detectors using the photon-photon coincidence technique. The experimental arrangement is shown in Fig. 6. The lifetime for the $1s2s\,^1S_0$ state is only 0.32 ps [68] so the detectors had to look directly at the exciter foil. The detectors looked at $60°$ with respect to the beam direction onto the back side of the target foil. Due to the high ion velocities this corresponds to emission angles of $90°$ in the ion rest frame, i.e., to a $180°$ back to back emission geometry for the two photons. In order to account for the angular dependent Doppler effect at the high ion energies used, granular X-ray detectors were used. On the right side of Fig. 6 a contour plot for events in which two photons were detected in coincidence is given. The diagonal feature corresponds to events for which the sum of the energies of
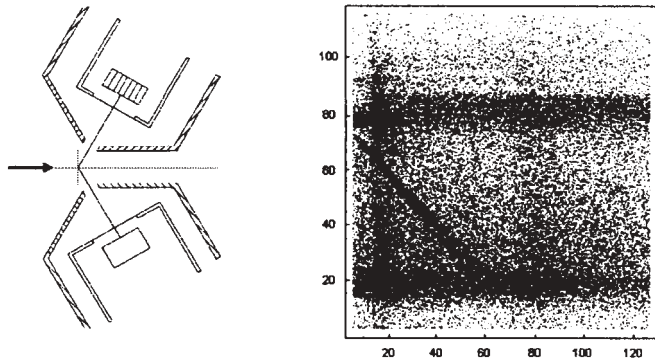
Fig. 6. Experimental arrangement for the two-photon decay experiment in Au. 106 MeV/u Au^{77+} ions are excited in an Al target foil. The two photons are detected in coincidence by two shielded Ge(i) X-ray detectors, where one is of granular structure. On the right side, coincidence events between the detectors are plotted. The axes give the X-ray energies (keV) of the coincident photons in the ion rest frame.

both photons is constant: these are the two-photon decay events.

The final result for the reduced matrix element in He-like Au^{77+} as a function of the energy fraction f is given in Fig. 7. A clear departure from the spectral distribution in Ni^{26+} was established confirming the full relativistic calculations of Derevianko and Johnson [68]. Still further data near the ends of the spectral distribution are needed for a more stringent test of two-photon decay in ions with strong central fields.

Recently a new method to efficiently produce the "metastable" $1s2s\,^1S_0$ state in heavy ions was introduced by Stöhlker and coworkers [79]. Li-like U ions at 217 MeV/u coasting in the heavy ion storage ring ESR at GSI in Darmstadt collided with nitrogen molecules at the internal gas jet target. By particle X-ray coincidence techniques only X-rays from singly ionized, i.e. from excited He-like ions were detected, cf. Fig. 8. At 217 MeV/u the projectile K-shell is predominantly ionized leaving the 2s electron untouched. Hence, by this specific ionization we end up predominantly in the excited $1s2s\,^3S_1$ and $1s2s\,^1S_0$ states of the He-like ions and only pure M1 and 2E1 X-ray transitions are observed, respectively. The spectral distribution for the two-photon decay is clearly observed
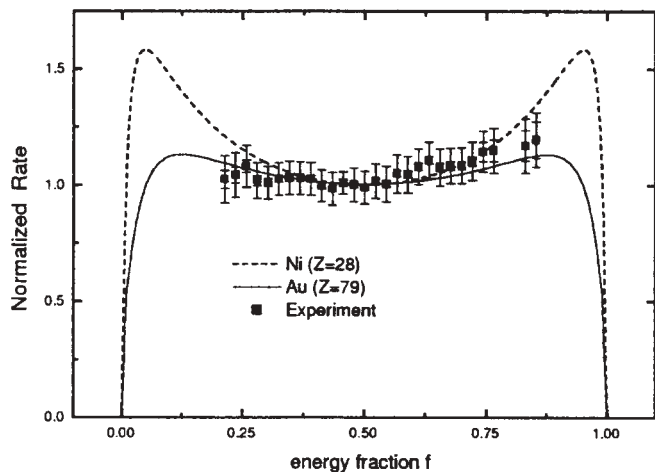

Fig. 7. Energy dependence of the reduced matrix element squared (normalized rate) extracted from the experiment compared to the fully relativistic theory for Au^{77+} and Ni^{26+} (full and dashed lines, respectively) [68].
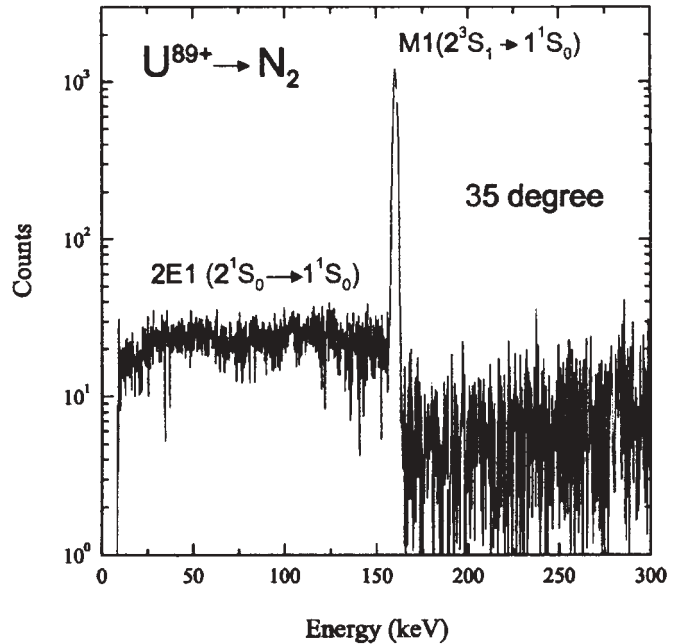
Fig. 8. X-ray spectrum registered with one detector at 35° to the beam direction and measured in coincidence with single ionization of initially Li-like U ions colliding at 378 MeV/u with nitrogen target atoms. Only events for the continuous two-photon decay spectrum and the M1 line emission from excited He-like U are observed.

without the need to additionally detect coincidences between the two photons.

3. Two-photon decay of inner-shell vacancies

In atomic systems with one K vacancy two-photon decay has to compete with the fast allowed decay modes in singly ionized atoms. Hence, the wings of the characteristic lines that are orders of magnitude larger heavily disturb the two-photon spectrum. Only a coincident detection of the two photons can discriminate against the tails of the characteristic lines. The first measurement for a heavy atomic system, Mo, was reported only in 1984, where the K vacancy was produced by photoionization [52]. A cleaner way to produce the inner-shell vacancy was introduced by Ilakovac and coworkers two years later [58]. They used a decay mode of radioactive nuclei, electron capture by the nucleus, for K-vacancy production. By detecting the two photons in coincidence they obtained clean two-photon spectra for the transitions 2s → 1s, 3s → 1s, 3d → 1s and 4s/d → 1s in xenon ($Z = 54$) [59], silver ($Z = 47$) and hafnium ($Z = 72$) [60]. All these measurements confirmed quite clearly the existence of the two-photon decay branch in singly ionized atoms—and demonstrated that all intermediate states have to be included in the summation whether they are occupied or empty. Moreover, a drastic difference in shape for the various two-photon decay branches, in particular for 2s → 1s and 3d → 1s transitions showing different phase space factors, was established.

Ilakovac and coworkers measured coincidences for back-to-back emission of the two photons. Schäffer and collaborators [80,81] reported measurements of the two-photon decay branches in Ag induced by nuclear electron capture, confirming with improved statistics the original findings of Ilakovac and his group. In Fig. 9 the 2E1
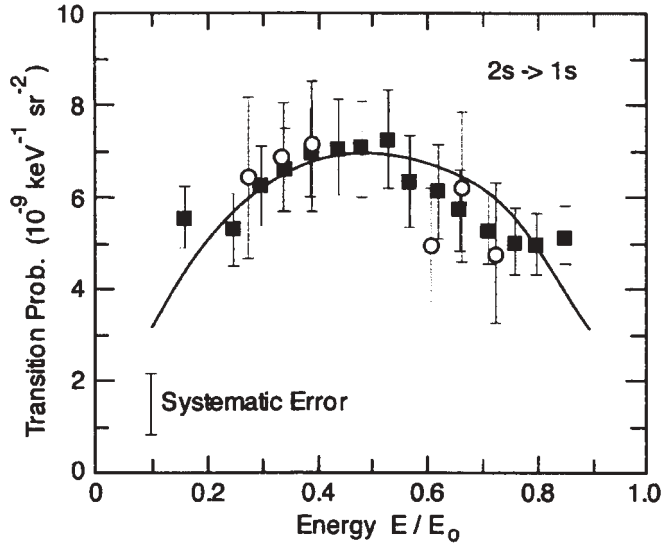
Fig. 9. The two-photon spectrum (transition probabilities) for singly K-ionized Ag atoms as function of the normalized photon energy; measurements from Refs. [60] (open circles) and [81] (full squares), theory according to Ref. [54] (curve).
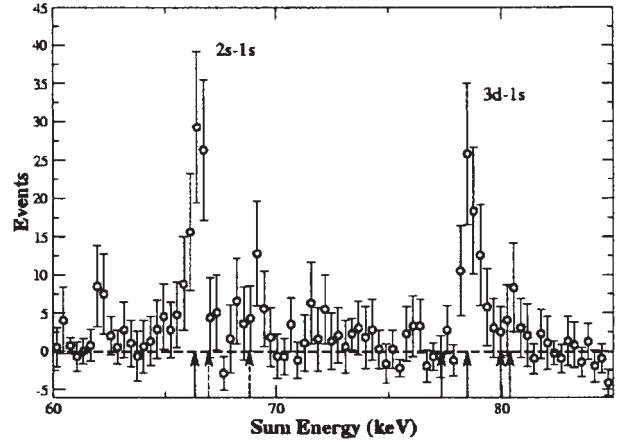

Fig. 10. Sum-energy spectrum of two-photon coincidence events after subtraction of random coincidences [82]. Solid arrows indicate the sum-energies corresponding to the $2s \to 1s$, $3s \to 1s$, $3d \to 1s$, $4s \to 1s$, and $4d \to 1s$ two-photon transitions for Au atoms with a single K vacancy. The dashed arrows show the positions of $K\alpha_1$ and $K\alpha_2$ transition energies [82].

transition probability per K vacancy decay in silver atoms is plotted as a function of the normalized transition energy; measurements of Ilakovac *et al.* [60] and Schäffer [81] are compared to theory [54].

The angular dependence of the two-photon emission was also probed by Schäffer and coworkers [80,81]. For $ns \to 1s$ transitions a $1 + \cos^2 \theta$ distribution is expected, and for $nd \to 1s$ transitions a $1 + (1/13)\cos^2 \theta$ distribution. Schäffer studied both $180°$ and $90°$ photon emission in order to confirm the difference in the angular distributions of these two transitions. The results are given in Table I. There is a reasonable agreement between experimental results [80,81] and theoretical values from Tong *et al.* [54].

An experiment at the Advanced Photon Source (APS) at Argonne National Laboratory has measured inner-shell two-photon decay in Au atoms [82]. In this measurement, the inner-shell vacancies were produced using X-rays from the bending magnet beamline 12-BM at the Basic Energy Sciences Synchrotron Radiation Center (BESSRC). The X-rays were incident on a $2\,\mathrm{mg/cm^2}$ Au target and passed on to a shielded beam dump located downstream of the target. Two shielded Ge detectors arranged in the polarization plane of the primary X-rays at $135°$ to the beam direction and $90°$ to each other detected X-rays from the target. Ta shields located between the two detectors suppressed "cross-talk" events caused by photons which Compton scatter in one detector crystal and are detected in the other. Such events produce coincidences with a sum energy equal to the energies of the diagram lines. Each of the detectors was surrounded by Pb and Pb walls were located in front of

and behind the target to cut down on background from scattered X-rays.

In Fig. 10 we show a sum-energy spectrum subject to the requirement that the individual photons in each detector lie within a 27 keV wide window centered at 33.2 keV (one half the $2s \to 1s$ transition energy). This region excludes photons from cascade transitions. The accidental coincidences have been subtracted from the prompt coincidences. The sum-energy spectrum shows two groups of lines. One group near 66 keV is associated with transitions from $n = 2$ to the ground state and the other near 78 keV is associated with transitions from $n = 3$ to the ground state.

In order to compare with theory we use the following relation (see Ref. [59]) to determine P, the triply differential two-photon transition probability normalized to the total transition probability W_K:

$$P = \frac{1}{W_K} \left(\frac{\mathrm{d}^3 w_{2\gamma}}{\hbar\, d\omega_1 \mathrm{d}\Omega_1 \mathrm{d}\Omega_2} \right)_{\theta=\pi/2} = \frac{\Delta n / \Delta E}{n_K \varepsilon_1 \varepsilon_2 \varepsilon_C \Delta\Omega_1 \Delta\Omega_2} \quad (9)$$

Here n_K is the number of K-holes produced in the experiment, Δn is the number of two-photon events in an energy interval ΔE, ε_j are the intrinsic photoefficiencies of the detectors, $\Delta\Omega_j$ are the solid angles of the detectors, ε_C is the efficiency of the coincidence electronics.

Although there have been no theoretical calculations for two-photon decay of inner shell vacancies in Au, we can learn something from a comparison with existing calculations done for lower-Z neutral atoms and calculations for two-photon decay in H-like ions. In Fig. 11 we summarize some of the data for the $3d \to 1s$ two-photon transition for the case of equal energy sharing and $\theta = \pi$. Experimental results are shown for silver ($Z = 47$), xenon ($Z = 54$), hafnium ($Z = 72$) and gold ($Z = 79$). For gold we have plotted the results of the experiment as well as this result multiplied by 14/13 to extrapolate to an opening angle $\theta = \pi$. The solid line is the theoretical result of Tong *et al.* [54] and the dashed line is the theoretical result of Mu and Crasemann [55] for the region from $Z = 42$ to 54. Although the solid curve fits the lower Z data better, both calculations indicate a positive slope at low Z whereas the experimental data are relatively flat as a function of Z.

Table I. *Intensity ratio* I*(180°)/*I*(90°) for the two-photon decay branches in Ag; experimental values from Ref. [80], theory according to Ref. [54].*

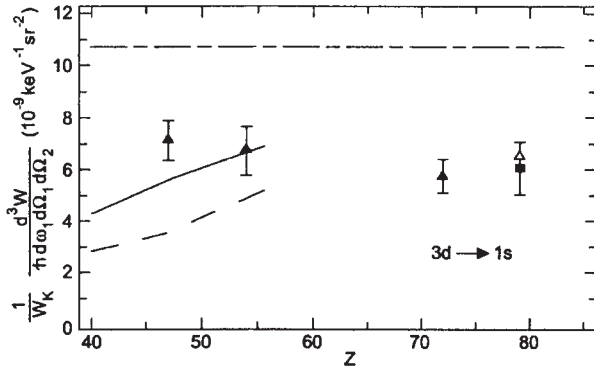| Transition	Experiment	Theory
$2s \to 1s$	1.90 ± 0.27	2.00
$3s \to 1s$	1.49 ± 0.34	2.00
$3d \to 1s$	1.22 ± 0.25	1.08

Fig. 11. Theoretical and experimental results for the triply differential transition probability for the two-photon transition $3d \rightarrow 1s$ normalized to the total transition probability W_K for decay of a K vacancy and plotted as a function of the nuclear charge Z [82]. Experimental results for $\omega_1 = \omega_2$ and $\theta = \pi$ are shown as solid triangles with error bars for silver ($Z = 47$) [60], xenon ($Z = 54$) [59] and hafnium ($Z = 72$) [60]. For gold the result of the present experiment ($\omega_1 = \omega_2$ and $\theta = \pi/2$) is shown as a solid square with error bars. The open triangle at $Z = 79$ is our gold result multiplied by 14/13 to extrapolate to an opening angle $\theta = \pi$. The solid curve shows the theoretical results of Tong *et al.* [54] and the dashed curve shows the results Mu and Crasemann [55] for the transition probabilities for $\omega_1 = \omega_2$ and $\theta = \pi$. The long-short dashed curve is the theoretical result of Florescu [15,16] for H-like ions at $\omega_1 = \omega_2$ and $\theta = \pi$. This result has been normalized using the transition probability for the 2p level in H-like ions and has been divided by 8 to fit on the plot [82].

For comparison, we also show the result of a non-relativistic calculation of Florescu for highly charged H-like ions (the dash-dot curve). In plotting these results we normalized to the decay rate of the 2p level in H-like ions. The resulting ratios are much larger than the neutral atom values and have been divided by a factor of 8 to fit them on the plot (which accounts roughly for the number of L electrons in the neutral atom). An interesting point is that at the level of the non-relativistic one-electron theory the differential two-photon decay rate is flat as a function of Z.

4. Conclusion

The experimental study of two-photon decay in heavy systems, i.e. for the strong field case has only begun. This process is sensitive to the complete structure of an atomic system as all occupied and unoccupied bound and unbound states contribute to this process. In this comment, the need for studying the spectral shape of the continuum emission in two-photon decay has been stressed. For highly-charged ions, not only do lifetime measurements provide less information, they are often impractical due to the very short lifetimes which characterize the two-photon emitting states in these systems. For He-like ions at intermediate Z, in particular for He-like nickel, the results are quite precise, yet there is a challenge to observe the relativistic effects which are most prominent in the wings of the spectral distribution function where issues of timing and detector efficiency pose problems. For very heavy He-like ions the results are presently less precise but there is no obstacle to improve the experimental accuracy for the spectral distribution. In particular the accuracies in the wings can be improved for heavy two-electron systems. This would give enhanced sensitivity to the complete structure of the ion for the strong field case. For very heavy He-like ions there is also a chance to observe the E1M1

decay of the $1s2s\,^3P_0$ state. With the beam foil technique the "prompt" 2E1 and "delayed" E1M1 decay can be clearly separated in that case.

The new technique developed at the ESR at GSI in Darmstadt to produce excited He- like ions by selective K ionization of Li-like fast heavy projectiles may give a quite new and exciting access to the two-photon spectra and hence to the complete structure of heavy He-like systems. Of particular interest is the fact that a continuum spectrum with very little background from other processes can be measured in a single Ge detector. This removes the complication of the need to understand the photon–photon coincidence efficiency which is the most difficult aspect of many of the experiments on two-photon decay.

For two-photon decay of inner-shell vacancies, the use of synchrotron radiation to produce singly K-ionized atomic systems provides a flexible tool to study the heaviest atomic systems. Now, all heavy atomic systems are accessible to structure investigations using the two-photon coincidence technique. Comparing two-photon data in singly K-ionized heavy atoms and He-like heavy ions will give additional insight into atomic structure and the changes due to additional electron interactions in a strong Coulomb field. In this case, the study of the spectral shape of the photon energy distributions provides a means of testing the theory. In particular these distributions could shed light on the question of the contribution of virtual electron–positron pairs which should contribute to the two-photon emission process at the highest Z. We also emphasize that theoretical calculations for two-photon decays in the heaviest neutral atoms are not available at present and such calculations would be of great interest particularly since high quality experimental data on these systems is now becoming available.

Looking further into the future, experiments to make more precise measurements of the opening angle distributions of two-photon decay are desirable. Such measurements provide a means of investigating the higher multipole contributions to two-photon decay, a point emphasized by Au [13]. These data would be of interest both for highly charged ions and for heavy neutral atoms. Beyond this, for two-photon decay of inner-shell vacancies, there is the additional question of how multi-electron dynamics affects the opening angle distributions. Moreover, we emphasize that hyperfine quenching may have to be considered in cases with non-zero spin for the electronic and nuclear states. Selecting an isotope with non-vanishing nuclear spin may reduce in He-like species the two-photon contributions from the decay of the $^3P_0$ state. These problems require progress in both experiment and theory.

Studies of two-photon decay have had a long history in physics. This inherently quantum mechanical process has provided a unique way to look at atomic structure (as well as nuclear structure) beyond the measurements of energy levels and lifetimes of single photon emitting states. In the future, we expect this window will continue to provide insights which will lead to a better understanding of atoms.

References

1. Göppert-Mayer, M., Ann. Phys. (Leipzig) **9**, 273 (1931).
2. Göppert, M., Naturwiss. **17**, 932 (1929).
3. Pagel, B. E. J., Nature **221**, 325 (1969).
4. Spitzer, L. Jr. and Greenstein, J. L., Astrophys. J. **114**, 407 (1951).
5. Breit, G. and Teller, E., Astrophys. J. **91**, 215 (1940).
6. Shapiro, J. and Breit, G., Phys. Rev. **113**, 179 (1959).
7. Zon, B. A. and Rapoport, L. P., Zh. Eksp. Teor. Fis. Pis'ma Red. **7**, 70 (1968); JETP Lett. **7**, 52 (1968).
8. Klarsfeld, S., Phys. Lett. **30A**, 382 (1969).
9. Klarsfeld, S., Lett. Nuovo Cimento **1**, 682 (1969).
10. Drake, G. W. F., Phys. Rev. A **34**, 2871 (1986).
11. Van Dyck, R. S. Jr., Johnson, C. E. and Shugart, H. A., Phys. Rev. A **4**, 1327 (1971).
12. Eichler, J., Phys. Rev. A **9**, 1762 (1974).
13. Au, C. K., Phys. Rev. A **14**, 531 (1976).
14. Tung, J. H., Ye, X. M., Salamo, G. J. and Chan, F. T., Phys. Rev. A **30**, 1175 (1984).
15. Florescu, V., Phys. Rev. A **30**, 2441 (1984).
16. Florescu, V., Patrascu, S. and Stoican, O., Phys. Rev. A **36**, 2155 (1987).
17. Bonin, K. D. and McIlrath, T. J., J. Opt. Soc. Am. B **1**, 52 (1984).
18. Dalgarno, A., Mon. Not. R. Astron. Soc. **131**, 311 (1966).
19. Dalgarno, A. and Victor, G. A., Proc. Phys. Soc. London **87**, 371 (1966).
20. Victor, G. A. and Dalgarno, A., Phys. Rev. Lett. **18**, 1105 (1967).
21. Victor, G. A., Proc. Phys. Soc. London **91**, 825 (1967).
22. Jacobs, V., Phys. Rev. A **4**, 939 (1971).
23. Drake, G. W. F., Victor, G. A. and Dalgarno, A., Phys. Rev. **180**, 25 (1969).
24. Bely, O., J. Phys. B **1**, 718 (1968).
25. Bely, O. and Faucher, P., Astron. Astrophys. **1**, 37 (1969).
26. Drake, G. W. F. and Dalgarno, A., Astrophys. J. **152**, L121 (1968).
27. DeMille, D., Budker, D., Derr, N. and Deveney, E., Phys. Rev. Lett. **83**, 3978 (1999).
28. Drake, G. W. F., Nucl. Instr. Meth. B **9**, 465 (1985).
29. Savukov, I. M. and Johnson, W. R., Phys. Rev. A **66**, 062507 (2002).
30. Dunford, R. W., to be published in Phys. Rev. A.
31. Schmieder, R. W., Phys. Rev. A **7**, 1458 (1973).
32. Novick, R., in "Physics of the One and Two Electron Atoms," (edited by F. Bopp and H. Kleinpoppen), (North Holland, Amsterdam, 1969), p. 296.
33. Lipeles, M., Novick, R. and Tolk, N., Phys. Rev. Lett. **15**, 690 (1965).
34. Arthur, C. J., Tolk, N. and Novick, R., Astrophys. J. Lett. **157**, L181 (1969).
35. Dunford, R. W. et al., Phys. Rev. Lett. **62**, 2809 (1989).
36. Marrus R. and Schmieder, R. W., Phys. Rev. A **5**, 1160 (1972).
37. Hinds, E. A., Clendenin, J. E. and Novick, R., Phys. Rev. A **17**, 670 (1978).
38. Gould, H. and Marrus, R., Phys. Rev. A **28**, 2001 (1983).
39. Prior, M. H., Phys. Rev. Lett. **29**, 611 (1972).
40. Cocke, C. L., Curnutte, B., Macdonald, J. R., Bednar, J. A. and Marrus, R., Phys. Rev. A **9**, 2242 (1974).
41. Kocher, C. A., Clendenin, J. E. and Novick, R., Phys. Rev. Lett. **29**, 615 (1972).
42. Cheng, S. et al., Phys. Rev. A **47**, 903 (1993).
43. Krüger, H. and Oed, A., Phys. Lett. **54A**, 251 (1975).
44. Dunford, R. W. et al., Phys. Rev. A **48**, 2729 (1993).
45. Simionovici, A. et al., Phys. Rev. A **48**, 1695 (1993).
46. Marrus, R. et al., Phys. Rev. Lett. **56**, 1683 (1986).
47. Pearl, A. S., Phys. Rev. Lett. **24**, 703 (1970).
48. Prior, M. H. and Shugart, H. A., Phys. Rev. Lett. **27**, 902 (1971).
49. Dunford, R. W. et al., Phys. Rev. A **48**, 1929 (1993).
50. Freund, I., Phys. Rev. A **7**, 1849 (1973).
51. Wu, Y.-J. and Li, J.-M., J. Phys. B **21**, 1509 (1988).
52. Bannett, Y. B. and Freund, I., Phys. Rev. A **30**, 299 (1984).
53. Åberg, T., in "Atomic Inner-Shell Processes," (edited by B. Crasemann), (Academic, New York, 1975), p. 353.
54. Tong, X.-M., Li, J.-M., Kissel, L. and Pratt, R. H., Phys. Rev. A **42**, 1442 (1990).
55. Mu, X. and Crasemann, B., Phys. Rev. A **38**, 4585 (1988).
56. Guo, D.-S., Phys. Rev. A **36**, 4267 (1987).
57. Bannett, Y. and Freund, I., Phys. Rev. Lett. **49**, 539 (1982).
58. Ilakovac, K., Tudoric-Ghemo, J. Busic, B. and Horvat, V., Phys. Rev. Lett. **56**, 2469 (1986).
59. Ilakovac, K., Tudoric-Ghemo, J. and Kaucic, S., Phys. Rev. A **44**, 7392 (1991).
60. Ilakovac, K. et al., Phys. Rev. A **46**, 132 (1992).
61. Schirmer, J. et al., Phys. Rev. Lett. **53**, 1897 (1984).
62. Kramp, J. et al., Nucl. Phys. A **474**, 412 (1987).
63. Goldman, S. P. and Drake, G. W. F., Phys. Rev. A **24**, 183 (1981).
64. Johnson, W. R., Phys. Rev. Lett. **29**, 1123 (1972).
65. Parpia, F. A. and Johnson, W. R., Phys. Rev. A **26**, 1142 (1982).
66. Goldman, S. P., Phys. Rev. A **40**, 1185 (1989).
67. Drake, G. W. F., unpublished report, University of Windsor (1988).
68. Derevianko, A. and Johnson, W. R., Phys. Rev. A **56**, 1288 (1997).
69. Elton, R. C., Palumbo, L. J. and Griem, H. R., Phys. Rev. Lett. **20**, 783 (1968).
70. O'Connell, D., Kollath, K. J., Duncan, A. J. and Kleinpoppen, H., J. Phys. B **8**, L214 (1975).
71. Schmieder, R. W. and Marrus, R., Phys. Rev. Lett. **25**, 1692 (1970).
72. Mokler, P. H. et al., Phys. Rev. Lett. **65**, 3108 (1990).
73. Stöhlker, T. et al., Phys. D **21**, S233 (1991).
74. Mokler, P. H., in "Recombination of Atomic Ions," (edited by W. G. Graham, W. Fritsch, Y. Hahn, and J. A. Tanis), NATO ASI (Plenum, New York, 1992), Vol. B **296**, p. 259.
75. Stöhlker, Th., internal report GSI-91–20 (1991).
76. Schäffer, H. W. et al., Phys. Rev. A **59**, 245 (1999).
77. Ali, R. et al., Phys. Rev. A **55**, 994 (1997).
78. Schäffer, H. W. et al., Phys. Lett. A **260**, 489 (1999).
79. Stöhlker T. et al., in "GSI Scientific Report 2000," (edited by U. Grundinger), (GSI, Darmstadt, 2001), Vol. 2001–1, p. 95; Banas D. et al., in "GSI Scientific Report 2002," (edited by U. Grundinger), (GSI, Darmstadt, 2001), GSI-report Vol. 2001–1, p. 88; Banas D. et al., to be published.
80. Mokler, P. H. and Dunford, R. W., Fizika A **10**, 105 (2001).
81. Schäffer, H. W., in "GSI-report Diss. 99-16," (1999).
82. Dunford, R. W. et al., Phys. Rev. A **67**, 054501 (2003).